

# Stress strain behavior research of triangular dam using analytical and numerical methods

*Maria Kozelskaya, Daria Donskova, Vera Ulianskaya\* and Pavel Shvetsov*

Don State Technical University, Rostov-on-Don, Russia

**Abstract.** The article deals with the calculation of triangular dams by numerical and analytical methods. The analytical solution is performed by a semi-inverse method. The stress function is taken as a polynomial of the third degree. Numerical calculation is performed using the finite element method. A comparison of the results obtained by the two methods is performed.

## 1 Introduction

Triangular shape dams are the one of the most economical structures in terms of materials consumption. Such structures must satisfy the following conditions: the absence of tensile stresses in the concrete, as well as the sufficient stability of the dam body against shear over the base. In order to respond enumerated requirements, it is necessary to make strength calculation of the specified structures. The determination of the stress-strain state of triangular dams can be performed by numerical and analytical methods of the theory of elasticity. In articles [1-5], a numerical solution of the plane problems of the theory of elasticity using the finite difference method is considered. For a triangular dam, use of this method is not possible. Finite element method (FEM) is more universal, which is used in the solution of mechanics two-dimensional problems of a deformable rigid solid in [6-14].

Comparison of stresses in a triangular dam obtained with FEM with the results of an analytical calculation will be implemented in this article.

## 2 Materials and methods

Triangular dam is considered, rigidly restrained at the base under the action of its own weight and hydrostatic pressure (Fig. 1). The height of dam  $h_0 = 3.2 \text{ m}$ , point angle  $\beta = 38^\circ$ , dam material specific gravity  $\rho = 20 \frac{\text{kN}}{\text{m}^3}$ , liquid specific gravity  $\gamma = 10 \frac{\text{kN}}{\text{m}^3}$

---

\* corresponding author: [vera@uliansky.com](mailto:vera@uliansky.com)

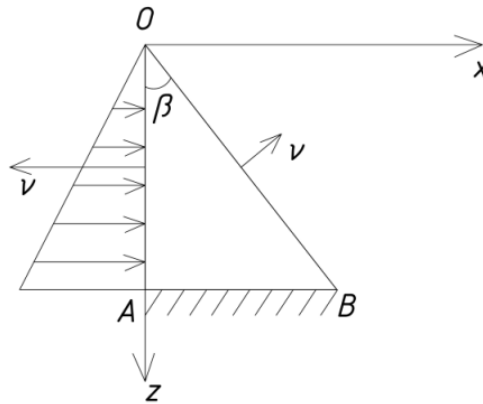


**Fig. 1.** Structural design

The basic resolving equation for the flat stress problem of the theory of elasticity is the biharmonic equation:

$$\frac{\partial^4 \varphi}{\partial x^4} + 2 \frac{\partial^4 \varphi}{\partial x^2 \partial z^2} + \frac{\partial^4 \varphi}{\partial z^4} = 0. \quad (1)$$

Stress function  $\varphi$  in accordance with [15] is taken in a form of polynomial with 4 undetermined coefficients  $A, B, C, D$ :

$$\varphi = \frac{A}{6}x^3 + \frac{B}{2}x^2z + \frac{C}{2}xz^2 + \frac{D}{6}z^3. \quad (2)$$

Stresses in dam are defined by formulas:

$$\begin{aligned} \sigma_x &= \frac{\partial^2 \varphi}{\partial z^2} = Cx + Dz; \\ \sigma_z &= \frac{\partial^2 \varphi}{\partial x^2} = Ax + Bz; \\ \tau_{xz} &= -\frac{\partial^2 \varphi}{\partial x \partial z} = -Xz - Zx = -Bx - Cz - \rho x \end{aligned} \quad (3)$$

where  $X$  и  $Z$  – components of volumetric load.

It is seems from formulas (3) that stresses are linear functions of coordinates with adjusted function  $\varphi$ .

The function (2) identically satisfies equation (1). Coefficients  $A, B, C, D$  are determined from the boundary conditions on faces  $OA$  and  $OB$ . Surface conditions are used for this, which have the form:

$$\begin{aligned} X_\nu &= \sigma_x \cdot l + \tau_{xz} \cdot n; \\ Z_\nu &= \tau_{zx} \cdot l + \sigma_z \cdot n, \end{aligned} \quad (4)$$

where  $l$  and  $n$  – directing cosines of the normal to the face,  $X_\nu$  и  $Z_\nu$  – components of surface load along  $x$  and  $z$  axes.

For  $OA$  face:

$$x = 0; l = \cos(x, \nu) = -1; n = \cos(z, \nu) = 0; X_\nu = \gamma z; Z_\nu = 0. \quad (5)$$

For  $OB$  face:

$$\begin{aligned} x = z \operatorname{tg} \beta; l = \cos(x, \nu) = \cos(\beta); n = \cos(z, \nu) = \cos(90^\circ + \beta) = \sin(\beta); \\ X_\nu = 0; Z_\nu = 0. \end{aligned} \quad (6)$$

Substituting (3), (5), (6) in (4), following stresses formulas will be obtained:

$$\begin{aligned} \sigma_x &= -\gamma z; \\ \sigma_z &= \left(-\frac{2\gamma}{tg^3\beta} + \frac{\rho}{tg\beta}\right) \cdot x + \left(\frac{\gamma}{tg^2\beta} - \rho\right) \cdot z; \\ \tau_{xz} &= -\left(\frac{\gamma}{tg^2\beta} - \rho\right) \cdot x - \rho x = -\frac{\gamma}{tg^2\beta} \cdot x. \end{aligned} \quad (7)$$

### 3 Results and discussion

The stress diagrams are shown in Fig.2 in the fixturing ( $z = 3.2$  m), calculated according to the formulas (7).

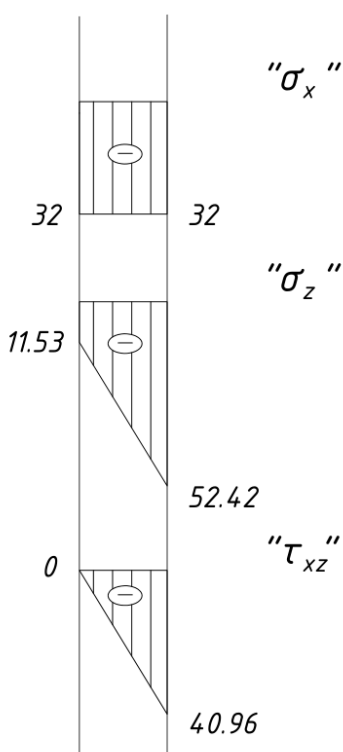


**Fig.2.** Stress diagrams in kPa for the reference zone that was analytically obtained

The calculation in software package LIRA-SAPR 2013 was made in two-dimensional setting (2 degrees of freedom). Flat triangular finite elements were used. Structural design is given in the Fig. 3.

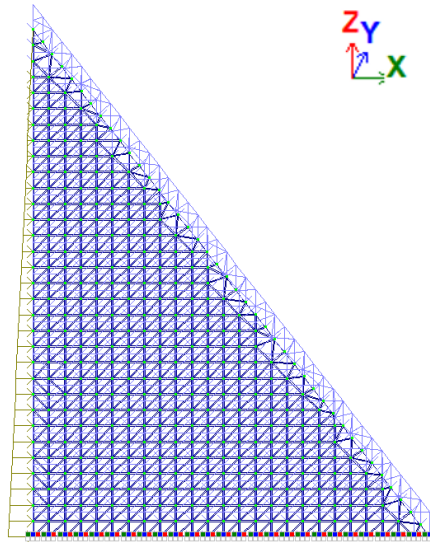


**Fig.3.** Structural design in LIRA-SAPR-2013 software package

Received stress isofields  $\sigma_x$ ,  $\sigma_z$  and  $\tau_{xz}$  are given on Figures 4-6.

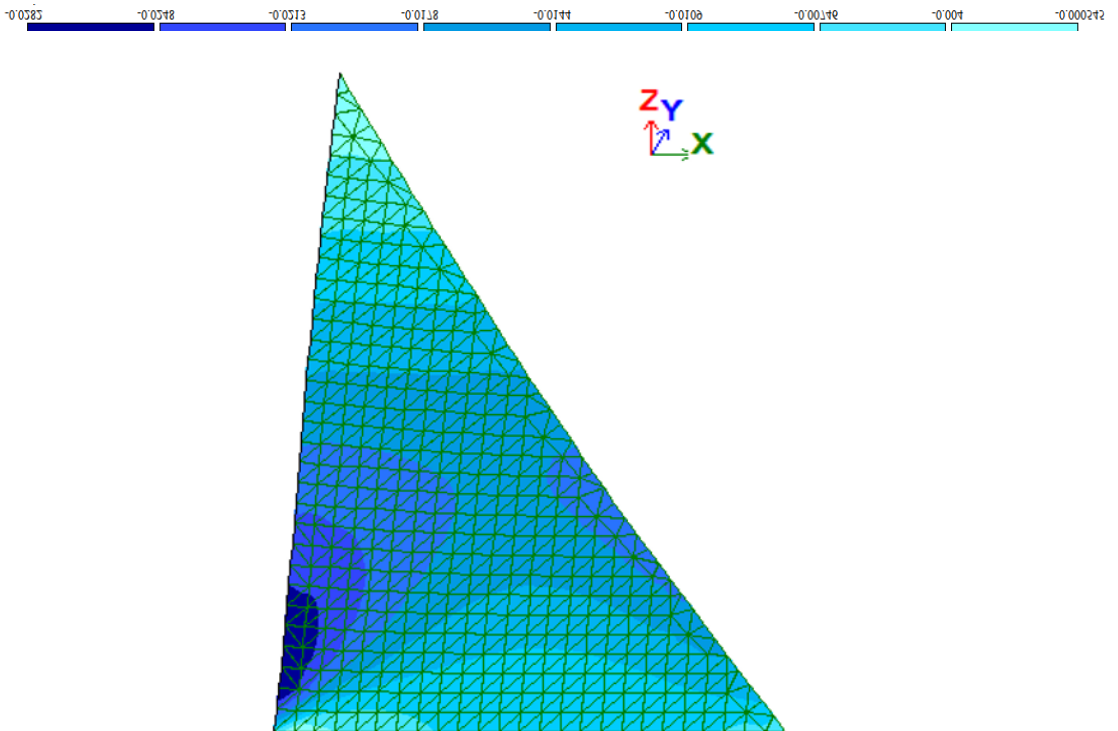


**Fig. 4.** Stress isofields  $\sigma_x$ , obtained in LIRA-SAPR

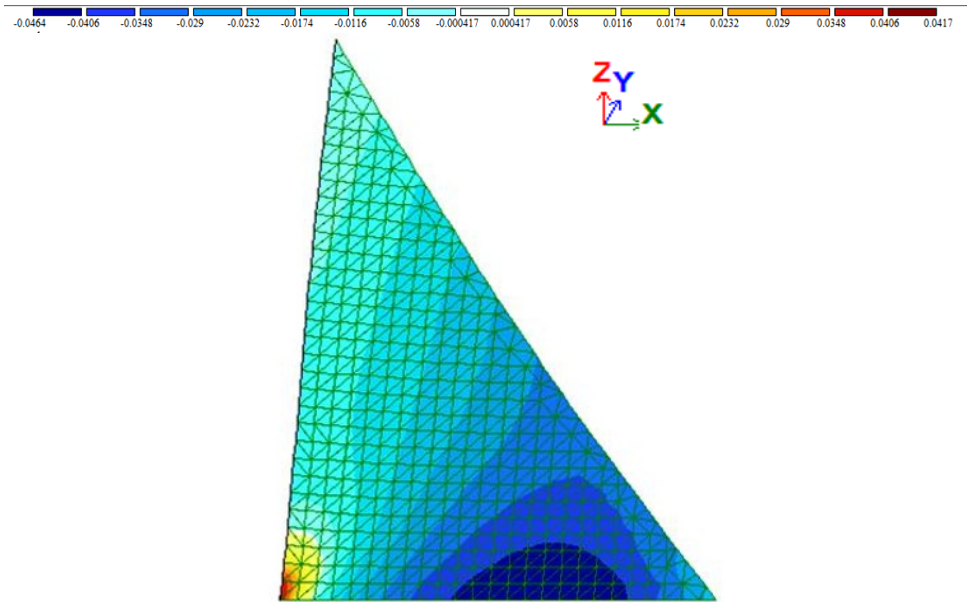


**Fig. 5.** Stress isofields  $\sigma_z$ , obtained in LIRA-SAPR

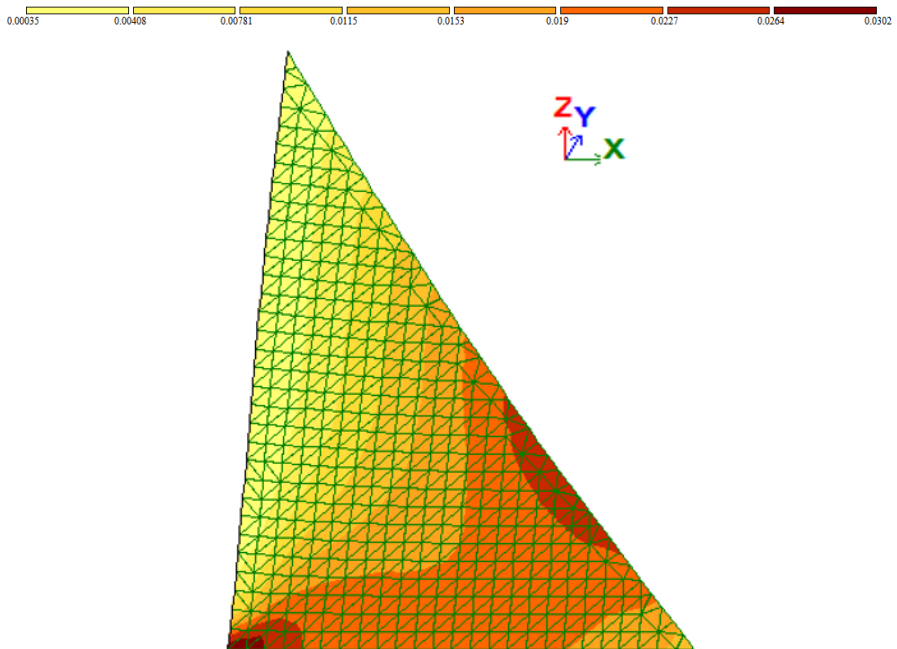


**Fig. 6.** Stress isofields  $\tau_{xz}$ , obtained in LIRA-SAPR

To compare the results with the analytical solution, stress diagrams were plotted in the  $z = 3.2$  m section (Figures 7-9).

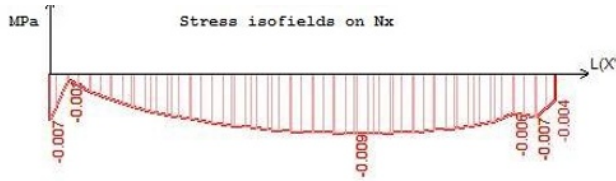


**Fig. 7.** Stress diagram  $\sigma_x$  with  $z = 3.2$  m (in the fixturing), obtained in LIRA-SAPR

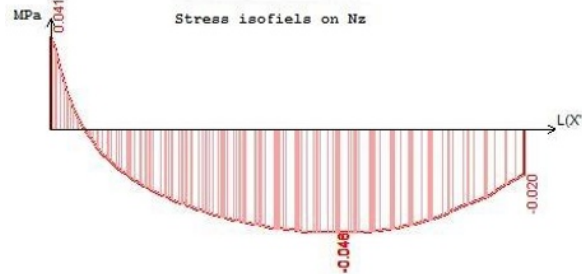


**Fig. 8.** Stress diagram  $\sigma_z$  with  $z = 3.2$  m (in the fixturing), obtained in LIRA-SAPR

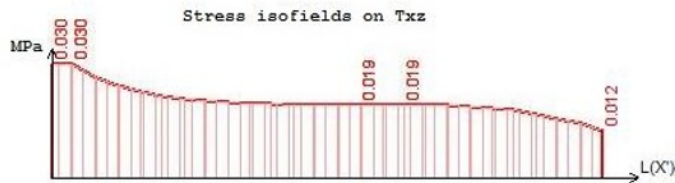


**Fig. 9.** Stress diagram  $\tau_{xz}$  with  $z = 3.2$  m (in the fixturing), obtained in LIRA-SAPR

Significant discrepancy of the results with the analytical solution can be seen from figures 7-9. Not only maximum stress values differ, but diagrams' character as well. This is due to the fact that the boundary conditions on the side AB were not considered while determining the constants A, B, C, D in the function (2).

At the same time, at points sufficiently remote from the reference zone, the solution by the methods of the classical theory of elasticity describes well enough the stress-strain state of the dam. Stress diagrams in the  $z = 1.6$  m section obtained in the LIRA program complex are given in Fig. 10-12. Fig. 13 shows the stress distribution in the same section in accordance with the analytical solution.

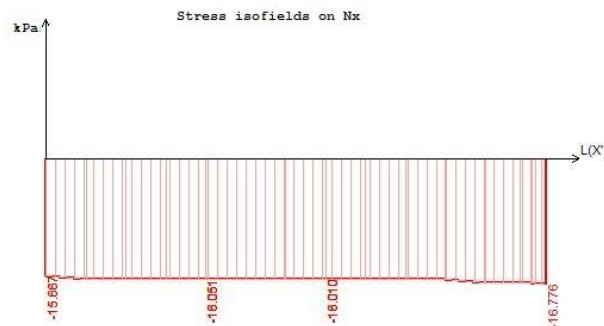


**Fig. 10.** Stress diagram  $\sigma_x$  with  $z = 1.6$  m, obtained in LIRA-SAPR

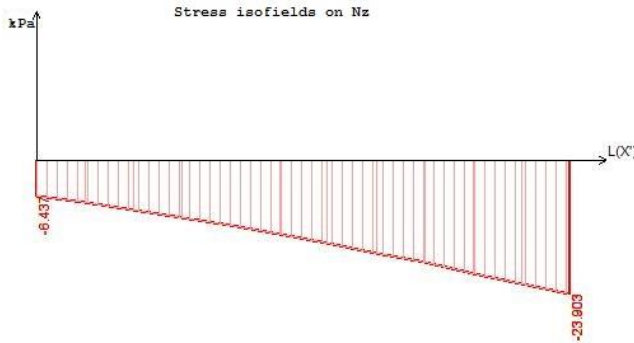


**Fig. 11.** Stress diagram  $\sigma_z$  with  $z = 1.6$  m, obtained in LIRA-SAPR

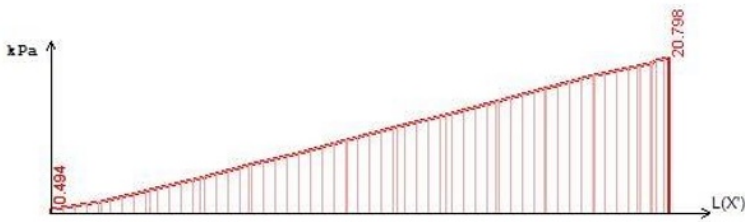


**Fig. 12.** Stress diagram  $\tau_{xz}$  with  $z = 1.6$  m, obtained in LIRA-SAPR

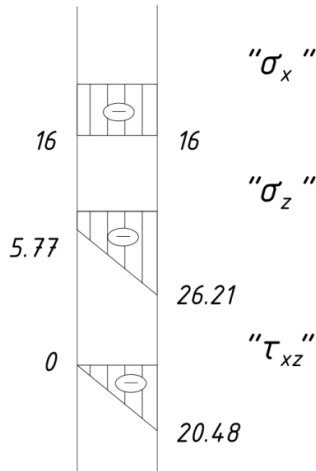


**Fig. 13.** Stress diagrams in kPa for the section  $z = 1.6$  m, obtained analytically

## 4 Conclusions

It can be seen from the presented graphs that the analytical solution based on the classical theory of elasticity describes quite well the stress-strain state of the structure at points, which are located far from the reference zone. The most dangerous zone is the support zone, which has a significant discrepancy between the results of the numerical and analytical solution. Thus, in the calculation and dams design, modern FEM systems are more recommended for use instead of analytical methods.

## References

1. V. I. Andreev, B. M. Yazyev, A. S. Chepurnenko, *Advanced Materials Research*, **900** (2014) 707-710
2. A.S. Chepurnenko, B.M. Yazyev, A.A. Savchenko, *Procedia Engineering*, **150** (2016) 1680–1685.
3. A.S. Chepurnenko, A.V. Saibel, B.M. Yazyev, *Procedia Engineering*, **150** (2016) 1694–1700.
4. L.R. Mailyan, A.S. Chepurnenko, A. Ivanov, *Procedia Engineering*, **165** (2016) 1853-1857.
5. V.I. Andreev, A.S. Chepurnenko, B.M. Jazyev, *Procedia Engineering*, **165** (2016) 1147–1151.
6. A.S. Chepurnenko, L.R. Mailyan, B.M. Jazyev, Calculation of the Three-layer Shell Taking into Account Creep, *Procedia Engineering*, **165** (2016) 990 – 994.
7. A.S. Chepurnenko, A.A. Savchenko, S.B. Yazyeva, *MATEC*, **129** (2017) 05008.
8. G.M. Danilova-Volkovskaya, A.S. Chepurnenko, A. Begak, A.A. Savchenko, *IOP Conference Series: Earth and Environmental Science*, **90** (2017).
9. A.A. Veremeenko, A.S. Chepurnenko, P.A. Shvetsov, L. A. Zorchenko, S.B. Yazyev, *IOP Conference Series: Earth and Environmental Science*, **90** (2017).
10. A.S. Chepurnenko, N.V. Neumerzhitskaya, and M.A. Turko // *Advances in Intelligent Systems and Computing*, **692** (2017) 808–818.
11. S. Litvinov, A. Zhuravlev, S. Bajramukov, S. Yazyev, *Advances in Intelligent Systems and Computing*, **692** (2017) 902-907.
12. L. Trush, S. Litvinov, N. Zakieva, S. Bayramukov, *Advances in Intelligent Systems and Computing*, **692** (2017) 885-893.
13. S. Litvinov, A. Beskopylny, L. Trush, S. Yazyev, *MATEC*, **106** (2017) 04013
14. S V. Litvinov, L. I. Trush, A. A. Avakov, 2017 International Conference on Industrial Engineering, Applications and Manufacturing (ICIEAM).
15. V. Samul. *Basics of theory of elasticity and plasticity* (Vysshaya shkola, 1982)